

# Filopodia formation and endosome clustering induced by mutant plus end-directed Myosin VI

Thomas A. Masters\* and Folma Buss\*

Cambridge Institute for Medical Research, University of Cambridge, Wellcome Trust / MRC Building, Hills Road, Cambridge, CB2 0XY

Submitted to Proceedings of the National Academy of Sciences of the United States of America

**Myosin VI (MYO6) is the only myosin known to move toward the minus end of actin filaments. It has roles in numerous cellular processes including maintenance of stereocilia structure, endocytosis and autophagosome maturation. However, the functional necessity of minus end-directed movement along actin is unclear as the underlying architecture of the local actin network is often unknown. To address this question, we engineered a mutant of MYO6, MYO6+, which undergoes plus end-directed movement whilst retaining physiological cargo interactions in the tail. Expression of this mutant motor in HeLa cells lead to a dramatic reorganization of cortical actin filaments and the formation of actin-rich filopodia. MYO6 is present on peripheral APPL1-positive signalling endosomes and MYO6+ expression causes a dramatic relocation and clustering of this endocytic compartment in the cell cortex. MYO6+ and its adaptor GIPC accumulate at the tips of these filopodia, whilst APPL1-positive endosomes accumulate at the base. A combination of MYO6+ mutagenesis and siRNA-mediated depletion of MYO6 binding partners, demonstrates that motor activity and binding to endosomal membranes mediated by GIPC and PI(4,5)P<sub>2</sub> are crucial for filopodia formation. A similar reorganization of actin is induced by a constitutive dimer of MYO6+ indicating that multimerization of MYO6 on endosomes through binding to GIPC is required for this cellular activity and regulation of actin network structure. This unique engineered MYO6+ offers insights into both filopodia formation and MYO6 motor function at endosomes and at the plasma membrane.**

Unconventional Myosins | Filopodia | Endosomes | Actin Dynamics

## Introduction

MYO6 is a monomeric motor protein with a large working stroke (1), which takes processive 36 nm steps along actin filaments in vitro when dimerized (2). Uniquely among myosin motors, it takes these steps toward the minus end of actin filaments (3). In cells and tissues, MYO6 has been implicated in an ever-growing list of functions including secretion, endocytosis, cell migration, stereocilia maintenance and autophagy (4). It mediates these functions through interactions with a wide array of cargo adaptor proteins that bind to the tail region of MYO6, thereby localising and potentially activating the motor through conformational change and unfolding of the lever arm (5) mediated by calcium (6). However, how the mechanical properties (for instance step size, duty ratio, stall force etc.) and in particular the directionality of MYO6 relate to its biological roles is poorly understood.

Isolated, purified MYO6 is primarily monomeric (1), but can dimerize in vitro through interactions between the cargo binding domain and adaptor molecules (2, 7). Whether any of these adaptors are capable of inducing functional MYO6 dimers in cells is not known and there has been little definitive evidence as to whether MYO6 functions as a monomer or as a processive dimer in cells and how motor processivity relates to its biological function (8, 9).

The cellular requirement for MYO6 to move toward the minus end of actin filaments is similarly poorly understood. The organization of the actin network at the plasma membrane, where plus ends are found adjacent to the membrane and minus ends toward the cytoplasm, implies MYO6 has a role in retrograde

transport along actin away from the plasma membrane. However, in other locations where a role for MYO6 has been identified, such as at the Golgi complex or nascent autophagosomes, the organization of the actin network is poorly characterized and it is far from obvious why a minus end motor would be required.

To begin to address these questions, we created a mutant of MYO6, MYO6+, which moves toward the plus end of actin filaments. Expression of this mutant in HeLa cells led to formation of filopodia, the reorganization cortical endosomes and of MYO6 adaptor proteins. This suggests that MYO6 may play a transient and highly regulated role in actin organization around endosomes underneath the plasma membrane and potentially at its other sites of function. We further validate the role of MYO6 in mediating the interaction of peripheral endosomes with the actin cortex, initiating movement away from the plasma membrane.

## Results

### *Expression of MYO6+ reorganizes actin at the plasma membrane*

To investigate the requirement of minus end directed movement of MYO6 for cellular function, we re-engineered MYO6 into a plus end directed motor by replacing the unique insert and neck regions with the myosin V lever arm (Figure 1A). Similar replacements in porcine MYO6 have been previously shown to lead to plus end-directed movement in vitro (10). When this construct was transfected into HeLa cells, we observed a dramatic reorganization of the actin cortex with formation of filopodia-like (11) protrusions of actin, where MYO6+ accumulated at the tips (Figure 1B). This is reminiscent of the previously reported accumulation of Myosin X (12) and dimeric Myosin VIIA (13) at tips of filopodia, indicating that MYO6+ was acting as a

## Significance

How the mechanical properties of myosin motors relate to their functions in cells is poorly understood. MYO6 is the only myosin that moves to the minus end of actin filaments, but the cellular requirement of this reverse movement is unknown. To investigate this question, we generated a mechanical mutant of MYO6, MYO6+, which moves to the plus end of actin filaments. This mutant causes clustering of signalling endosomes coupled to reorganization of cortical actin filaments into elongated filopodia. These two phenotypes depend on the multimerization of MYO6+ on the endosomal membrane induced by binding to lipids and adaptor proteins. Our results highlight the importance of endosomes for myosin-dependent regulation of cortical actin filaments in mammalian cells.

## Reserved for Publication Footnotes

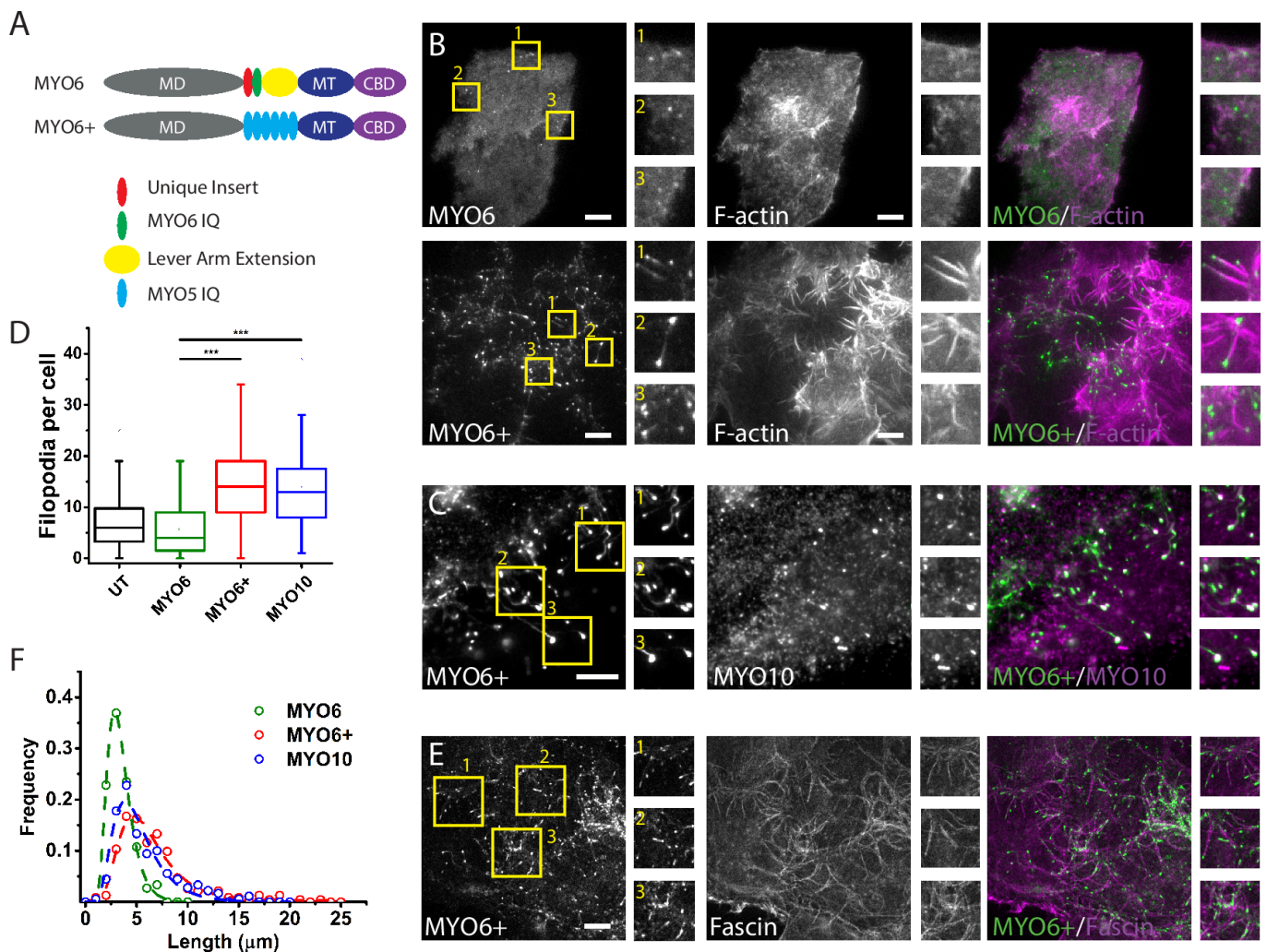


**Fig. 1.** Expression of MYO6+ leads to formation of elongated filopodia. **A**) Constructs used in this study (MD – motor domain, MT – medial tail, CBD – cargo binding domain). **B**) TIRF images of HeLa cells expressing either GFP-MYO6 (top panel) or GFP-MYO6+ (lower panel) showing formation of filopodia, which extend across the coverslip surface. Insets shown are 8x magnification. **C**) TIRF image showing colocalization of MYO6+ and MYO10 at the tips of filopodia. Insets shown are 4x magnification. **D**) Box-and-whisker of the number of filopodia in cells either untransfected or expressing the indicated GFP-tagged constructs (more than 60 cells per construct over 3 independent experiments). Stars indicated  $p < 0.001$ . **E**) TIRF image showing MYO6+ at the tips of fascin bundles. Insets shown are 4.5x magnification. **F**) Normalized distribution of filopodia length in cells expressing GFP-MYO6 (black circles, 149 cells, 3 experiments), GFP-MYO6+ (blue circles, 233 cells, 3 experiments) or GFP-MYO10 (red circles, 180 cells, 3 experiments). Errors shown are SEM. Scale bars 10  $\mu$ m.

processive plus end-directed motor in cells. A shorter replacement of the unique MYO6 neck region with only 2 IQ motifs (retaining the lever arm extension) led to a similar formation of filopodia (Figure S1). To confirm whether MYO6+ was indeed accumulating at actin filament plus-ends, we co-transfected GFP-MYO6+ with MYO10-mCherry (Figure 1C). MYO6+ was observed to colocalise with MYO10, a protein known to induce filopodia and accumulate at filopodia tips (12). MYO6+ had a similar propensity to induce filopodia as MYO10 in HeLa cells (Figure 1D), indicating that MYO6+ was functioning in a similar capacity. The actin-rich protrusions induced by MYO6+ were positive for fascin along the shaft (Figure 1E), indicating they are indeed filopodia. We extracted the lengths of filopodia from TIRF images and found they adopted a log-normal distribution (Figure 1F), as previously reported for both filopodia (14) and neuronal spines (15). The mode length of this distribution is  $5.66 \pm 0.14 \mu$ m as compared to  $3.22 \pm 0.04 \mu$ m in cells transfected with GFP-MYO6. The average length of filopodia in cells expressing GFP-MYO6+ is  $6.3 \pm 3.7 \mu$ m (S.D.,  $n = 233$ ) as compared to  $2.95 \pm 1.1 \mu$ m (S.D.,  $n = 149$ ) in cells expressing wild type GFP-MYO6 ( $p < 0.0001$ ) and  $5.3 \pm 2.9 \mu$ m (S.D.,  $n = 180$ ) in cells

expressing GFP-MYO10 (in agreement with a previous report (12)), indicating the activity of MYO6+ is capable of significantly increasing the length of filopodia. To assess the requirement for endogenous MYO6 in this process, we expressed MYO6+ in HeLa cells rendered null for MYO6 by modification with CRISPR/Cas9 (16). We found no difference in the propensity of GFP-MYO6+ to induce filopodia in these cells compare to wild type HeLa cells, indicating that indeed expression of MYO6+ alone leads to the formation and elongation of filopodia with MYO6+ localized to the tip (Figure S1C). Expression of GFP-MYO6+ did not affect the level of endogenous MYO6 (Figure S1D).

#### Expression of MYO6+ reorganizes MYO6 binding partners and signalling endosomes

Given that MYO6+ dramatically reorganized cortical actin structures and displayed a very different localization as compared to MYO6, we examined the distribution of well-characterized MYO6 binding partners. The endosomal protein GIPC (GAIP-interacting protein, C terminus (17)), which typically co-localizes with MYO6 on APPL1-positive signalling endosomes at the cell periphery, accumulated with MYO6+ at the tips of filopodia (Figure S2A). In contrast, the endosomes themselves, as detected



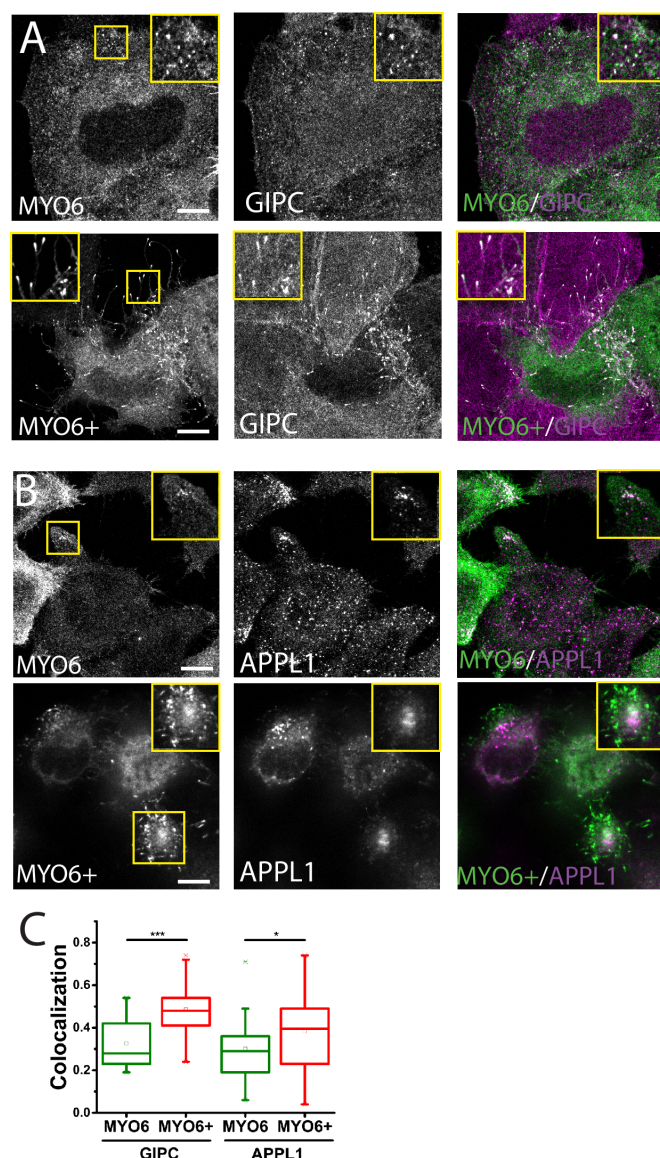


**Fig. 2.** Endosomal MYO6 binding partners are reorganized by MYO6+. A) HeLa cells were transfected with GFP-MYO6 or GFP-MYO6+, fixed, stained for GIPC and imaged by confocal microscopy. B) HeLa cells were transfected with GFP-MYO6 or GFP-MYO6+, fixed, stained for APPL1 and imaged by confocal microscopy (scale bars 10  $\mu$ m). C) Pearson's correlation coefficients were calculated for cells expressing either MYO6 or MYO6+ and stained with anti-GIPC or anti-APPL1 as indicated (more than 30 cells from 3 independent experiments).

with an antibody against APPL1, clustered at the base of the filopodia (Figure S2B). This indicates that APPL1 endosomes are guided to the base of the filopodia by MYO6+/GIPC complexes, but are unable to move into the filopodial shaft as it is tightly packed with protein and surrounded by membrane. MYO6+/GIPC complexes then detach from these endosomes and move toward the filopodia tips. Examining these structures by Structured Illumination Microscopy (SIM), we observed many of these tips were apparently extended and curved (Figure S2A). Furthermore, APPL1 endosomes clustered in an actin rich region from which filopodia emanate (Figure S2B).

Interestingly, the MYO6 endosomal binding partner TOM1 (18) can only accumulate at the base of filopodia but not at the tips (Figure S3A), indicating it does not detach from signalling endosomes. MYO6 and its binding partners often undergo transient

interactions, which are difficult to observe in cells. Intriguingly, MYO6+ is able to sequester a selection of binding partners at the tips of filopodia, spatially segregating these complexes at the plasma membrane. In particular, MYO6+ is able to recruit TAX1BP1 (19), and DOCK 7 (20) into newly formed filopodia (Figure S3B), whereas optineurin (21) and NDP52 (19) were not relocated. (Figure S3C). This was quantified by comparing Pearson's correlation coefficients between cells expressing either GFP-MYO6 or GFP-MYO6+ (Figure S3D). Thus, MYO6+ may prove to be a useful tool to interrogate the properties of various MYO6 binding partner complexes in intact cells via fluorescence imaging.

#### *MYO6+ requires the RRL and PI(4,5)P<sub>2</sub> binding sites and normal actin kinetics to form filopodia*

Given that MYO6+ was able to relocate its binding partners, we examined whether sites in the MYO6 tail known to mediate interactions with adaptor proteins (4) were important for filopodia formation and the translocation of MYO6+ to filopodia tips. Mutation of either the RRL motif (R1117L, known to co-ordinate interactions with GIPC, TAX1BP1, NDP52 and optineurin) or the PI(4,5)P<sub>2</sub> interacting motif in the tail of MYO6+ led to a dramatic reduction in the accumulation of MYO6+ at the tips of filopodia (Figures 3A, B). In contrast, mutation of the WWY site (W1202L, which binds to DAB2, TOM1 and LMTK2, Figures 3A, B) or the ubiquitin binding site (A1013G) have no effect on this accumulation. Thus, the RRL site appears to be the key site for formation of the processive (multimeric) form of MYO6 in cells. To test whether processive movement on actin is required, we made mutations in the motor domain of MYO6+. The rigor mutant K157R, which is unable to bind ATP and so remains tightly bound to actin, also prevented accumulation in filopodia (Figure 3A, B). A mutation (D179Y), which has been shown to accelerate phosphate release from MYO6 and thereby prevents processive runs on actin (the mutation increases the rate of phosphate release prior to actin binding) (22), also leads to a complete loss of MYO6+ induced filopodia (Figure 3A, B). Thus, processive movement on actin is required for accumulation of MYO6+ at the tips of filopodia. In contrast, mutation of the putative phosphorylation site in the motor domain Thr405 (23), to either alanine or glutamic acid, had no effect on filopodia formation.

#### *MYO6+ functions on signalling endosomes*

As only a specific subset of tail motifs was required for filopodia formation and only certain binding partners were reorganized by MYO6+, we next examined the role of these partners in the capacity of MYO6+ to induce filopodia. Knockdown of the endosomal protein GIPC (Figure 4A, B, C) led to a dramatic reduction in the number of cells with filopodia induced by MYO6+. Likewise, ablation of the characteristic marker of signalling endosomes, the GIPC-binding partner APPL1, displaced GIPC from endosomes and prevented accumulation of MYO6+ at tips of filopodia (Figure 4A, B, C). In contrast, depletion of either NDP52 or DOCK7 had no effect on filopodia formation and movement of MYO6+ to tips of filopodia (Figure 4B). When APPL1 was depleted, GIPC became cytosolic but was still stable and not degraded (Figure 4D). However, MYO6+ no longer induces formation of filopodia, indicating that the MYO6 tail can only interact with GIPC on endosomes. This is consistent with the requirement for an intact PI(4,5)P<sub>2</sub> binding site in the MYO6 tail to ensure membrane binding.

To further probe the requirement for processive movement in formation of filopodia, we transfected cells with a CBD-tail-less version of MYO6+, which was constitutively dimerized by inclusion of a leucine zipper at the C-terminus (Figure 4E). Expression of a leucine zippered MYO6+ lacking the CBD-tail still led to the formation of filopodia, but without recruitment of GIPC into the tips and without clustering of endosomes at the

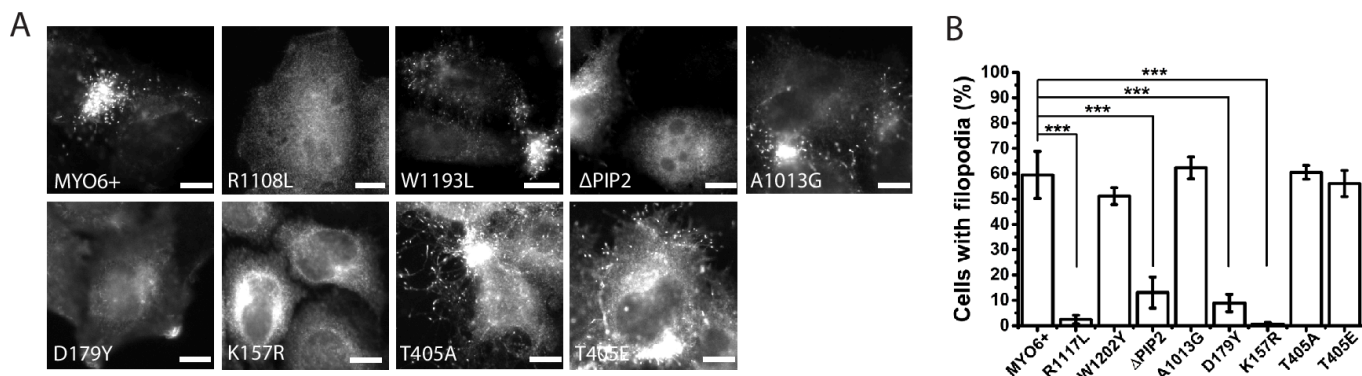


**Fig. 3. Mutations of MYO6 residues within MYO6+ disrupt filopodia formation.** A) HeLa cells were transfected with GFP-MYO6+ control, or with point mutations at specific sites in the MYO6 motor domain (D179Y, K157R, T405A and T405E) or tail (R1108L to ablate RRL binding site; W1193L to ablate WWY binding site;  $\Delta$ PIP2; A1013G) of MYO6+ as specified in the panels, fixed and stained with 568-phalloidin and imaged by widefield microscopy. B) Images in A (MYO6+ wild type or head and tail mutants) were quantified by counting the percentage of transfected (GFP-positive) cells presenting GFP-MYO6+ at the tips of filopodia (data are aggregate of 3 experiments with at least 50 cells per experiment, errors shown are SEM, p values for two-sample t-tests with the wild-type are R1108L  $p < 0.001$ , W1193L  $p = 0.12$  (not significant),  $\Delta$ PIP2  $p < 0.001$ , A1013G  $p = 0.58$  (not significant), D179Y  $p < 0.001$ , K157R  $p < 0.001$ , T405A  $p = 0.83$  (not significant) and T405E  $p = 0.57$  (not significant)). Scale bars 20  $\mu$ m.

base of filopodia (Figure 4F, S3). Further deletion of the leucine zipper led to a cytoplasmic construct (Figure S4). This indicates that key to the formation of filopodia is the multimerization of MYO6+, by assembly of at least a dimer. Furthermore, this experiment indicates that assembly of processive complexes of MYO6 requires targeting to endosomes.

#### Dynamic organization of MYO6+ induced filopodia

To investigate the processes underlying formation of filopodia by expression of MYO6+, we used live-cell TIRF microscopy to observe growing filopodia. By co-expressing GFP-MYO6+ and Ruby-lifeact (to detect F-actin), growing filopodia could be identified (Figure 5A, B, Movie S1). The average rate of growth of a filopodia tip was  $0.63 \pm 0.02 \mu\text{m min}^{-1}$  (SEM,  $n = 228$ ) similar to the previously reported rate of actin polymerization in filopodia ( $0.5 - 1 \mu\text{m min}^{-1}$ ) (24) and about 5-10 times slower than the rate that MYO6 can slide actin filaments in vitro (1). In addition to growth we also frequently observed movement of GFP-MYO6+ patches away from the filopodia tips toward the base (Figure 5C, D, Movie S2) at an average speed of  $0.99 \pm 0.09 \mu\text{m min}^{-1}$  (SEM,  $n = 62$ ), again similar to the rate of actin polymerization in cells (Figure 5E). Although most of the MYO6+ accumulates at the tips of filopodia, it forms long lasting complexes with actin and thus can be transported through actin filament treadmill towards the base of filopodia (opposite to their direction of motion).

In addition to simple growth and retrograde movement, the filopodia were capable of more complex dynamics including wave propagation (Figure 5F). These waves have a wavelength of  $2.27 \mu\text{m} \pm 0.18 \mu\text{m}$  (the distribution is shown in Figure 5G, SEM,  $n = 20$ ) and propagate at a speed of  $1.18 \pm 0.09 \mu\text{m min}^{-1}$  (Figure 5H, SEM,  $n = 39$ ), again very similar to the rate of actin treadmill. On some occasions complete twisting of the wave into a coil was observed (Figure S5A, B). Filopodia were also capable of splitting at the head (Figure S5C, D).

We next analysed whether MYO6+ induced the formation of filopodia by recruiting or activating proteins regulating actin organisation (Figure S6A). We did not observe a significant effect of depleting Arp3, mDia2 or N-WASP (shown in Figure S6E) on the percentage of cells with MYO6+ induced filopodia (Figure S6A, B). Depletion of Arp3 in cells transfected with GFP-MYO6+, and thus reduced actin branching, led to the formation of slightly more transfected cells forming filopodia (Figure S6B), and longer individual filopodia (of mean length  $13.3 \pm 6.5 \mu\text{m}$  S.D.,  $n = 215$  from 3 experiments, vs  $6.6 \pm 3.8 \mu\text{m}$  S.D.,  $n = 174$  from 3 experiments,  $p < 0.0001$ , Figure S5C). However, Arp3 de-

pletion significantly reduced the propensity of filopodia induced by MYO6+ to themselves form clusters (Figure S6D, that are not observed for MYO10 which does not require endosomes to promote filopodia formation). This indicates that Arp2/3-induced network branching is important for the reorganization of the actin cortex and the clustering of peripheral endosomes. Depletion of the formin mDia2 had no effect on filopodia induced by either MYO6+ or MYO10. Whilst depletion of N-WASP had a limited effect on MYO6+ induced filopodia, depletion of N-WASP led to a marked reduction in filopodia formation by MYO10 indicating that differences exist in the mechanism of filopodia formation between the two motors. In summary our data indicate that formation of filopodia by MYO6+ is a robust phenotype that depends on motor activity and cargo-mediated multimerization, but does not involve the established actin polymerization machinery.

#### Discussion

We set out to address the cellular requirement of minus end-directed translocation of MYO6 by cloning and expression of MYO6+, a plus end-directed MYO6 mutant. Expression of GFP-MYO6+ led to formation of numerous filopodia with GFP-MYO6+ and its binding partner GIPC localized at the tips, whilst endosomes, their site of interaction, accumulated in the actin cortex at the base of the filopodia. Filopodia formation depended on GIPC and its membrane anchor APPL1, but not on other endosomal binding partners such as TOM1. Mutations in residues crucial for ATPase activity, cargo or membrane binding prevented this process. Formation of filopodia could be recapitulated by forced dimerization of MYO6+ lacking the cargo binding tail, indicating that both crosslinking of actin filaments and processive movement along them by two or more actin-binding motor domains was crucial for actin reorganization. Taken together, these results indicate that MYO6 binds to APPL1 endosomes through GIPC, requiring both the RRL and PI(4,5)P<sub>2</sub> sites. MYO6 bound to GIPC on endosomes is functionally equivalent to a dimer or multimer, in contrast to TOM1-bound complexes that may exist as a monomer and thus may have a different functional role. The importance of endosomal targeting to achieve multimerization confirms previous studies which demonstrated that vesicle-associated MYO6 can exist as a dimer or multimer (25). These results are summarized in our model (Figure S7).

The binding of MYO6+ to GIPC on endosomes leads to formation of higher-order complexes and movement of MYO6+ towards actin filament plus ends at the plasma membrane. Such movements on the underlying network architecture induce endo-



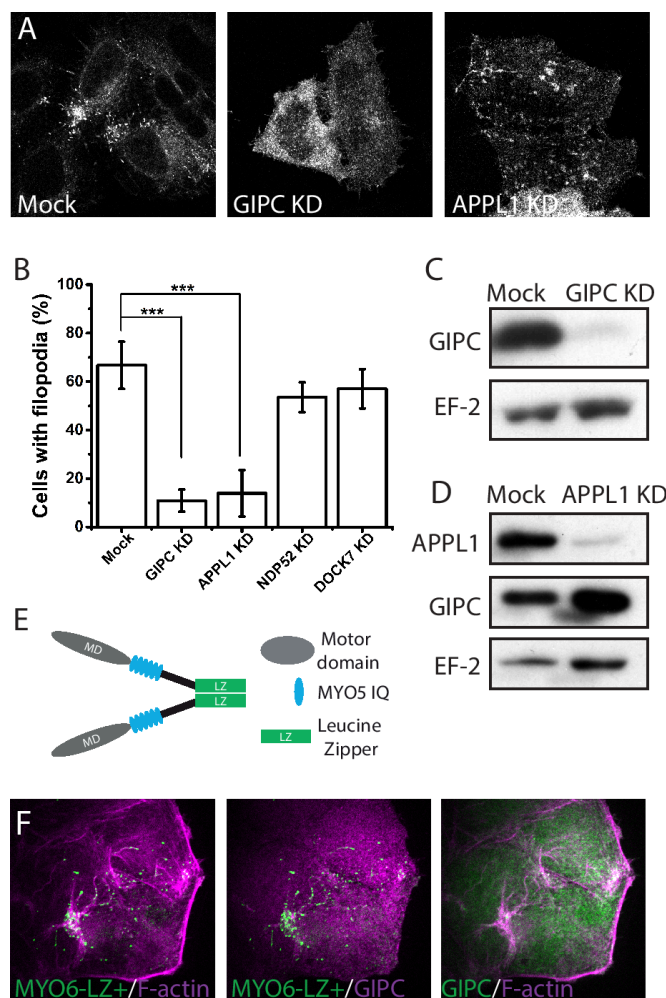


**Fig. 4.** APPL1 positive endosomes are required for formation of filopodia by MYO6+. A) HeLa cells were transfected with GIPC or APPL1 siRNA, transfected with GFP-MYO6+, fixed and imaged by confocal microscopy. B) Quantification of MYO6+ accumulation in filopodia tips (data are aggregate of at least 3 experiments with over 200 cells counted per condition). Respective p values are GIPC KD  $p < 0.001$ , APPL1 KD  $p < 0.001$ , NDP52 KD  $p = 0.11$  (not significant), DOCK7 KD  $p = 0.17$  (not significant). C) Western blots showing knockdown efficiency for GIPC, with EF-2 as loading control. D) Knockdown of APPL1 does not cause degradation of GIPC. E) Schematic of GFP-MYO6-LZ+, a leucine zippered MYO6+ HMM lacking the cargo binding tail. F) Cells were transfected with GFP-MYO6-LZ+, fixed, stained with anti-GIPC and phalloidin (for F-actin), and imaged by confocal microscopy. Scale bars 10  $\mu\text{m}$ .

some clustering at the plasma membrane. Continued active movements of MYO6+ dimers lead to actin filament condensation, filopodia formation and elongation. MYO6+ and its associated adaptor proteins migrate along actin filaments towards the tips, whereas APPL1 endosomes are retained in an actin meshwork at the base of the filopodia.

#### Actin organization by MYO6

Increasing evidence indicates that myosin motors not only use actin as a track, but can also organize actin filaments. In vitro, MYO6 in a zippered-dimer format can bundle arrays of filaments on a timescale of minutes to hours (26). In vivo, actin organization has been shown to require MYO6 in *Drosophila* spermatid individualization (27), at cell-cell junctions (28) and on melanosomes (29). GIPC has been identified as having a role in maintaining actin structures in hair cells (30), indicating that the actin organising function of MYO6 operates through GIPC on endosomal membranes. In the present study, nascent actin

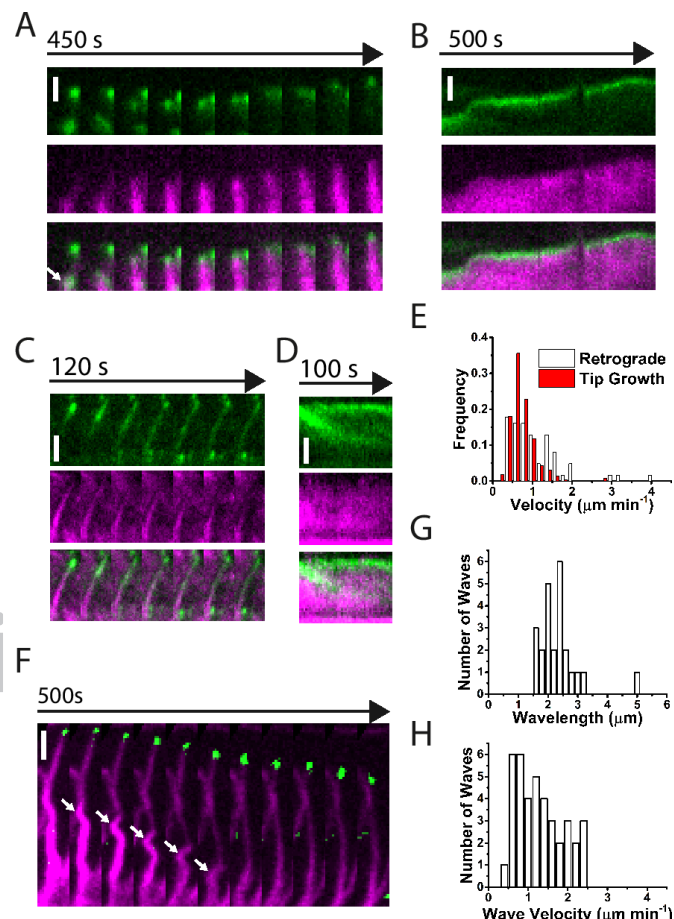


**Fig. 5.** Analysis of filopodia dynamics. A) Image sequence showing a growing filopodia tip imaged by TIRF microscopy (MYO6+ in green; F-actin probe lifeact in magenta; scale bar 1  $\mu\text{m}$ , 50 s per frame), white arrow indicates growing tip. See also Supplementary Movie S1. B) Kymographs of image sequence in A (MYO6+, green; lifeact, magenta; scale bar 1  $\mu\text{m}$ , 5 s per pixel). C) Image sequence of retrograde movement away from filopodia tips (MYO6+, green; lifeact, magenta; scale bar 2  $\mu\text{m}$ , 20 s per frame). See also Supplementary Movie S2. D) Kymographs of image sequence in C (MYO6+, green; lifeact, magenta; scale bar 2  $\mu\text{m}$ , 2 s per pixel). E) Histogram plots quantifying A and B. F) Image sequence showing retrograde wave movement in filopodia (MYO6+, green; lifeact, magenta; scale bar 2  $\mu\text{m}$ , 50 s per frame), the white arrow indicates a travelling wavefront. See also Supplementary Movie S3. G) Histogram of wavelengths. H) Histogram of wave velocities.

filaments formed by MYO6+ activity were apparently stabilized by the accumulation of fascin (Figure 1E). Thus the action of actin-associated motor proteins can also affect the recruitment and activity of actin regulators. The underlying mechanism may operate in concert with selective recruitment of tropomyosin isoforms which can serve to specify actin filament identity (31).

Interestingly, we also observed rotational waves and coiling within MYO6+ induced filopodia (Figure 5). Travelling waves along filopodia have been recently described by a helical buckling model (32). This was hypothesized to require a rotational force at one end and a fixed point at the other end of the filopodia. We propose that a rotation could also be generated by the coupling of MYO6+ to both the filopodial membrane through binding to PI(4,5)P<sub>2</sub> and actin through the motor domain. Consistent with this notion, helical movement of MYO6 around actin filaments has been reported in vitro (33). Furthermore, the hook-like shape of the tips of MYO6+ filopodia, as observed in our SIM images (Figure 2), may indicate that the accumulation of a high density of MYO6+ motors at the tip may exert significant bending or tor-

681  
682  
683  
684  
685  
686  
687  
688  
689  
690  
691  
692  
693  
694  
695  
696  
697  
698  
699  
700  
701  
702  
703  
704  
705  
706  
707  
708  
709  
710  
711  
712  
713  
714  
715  
716  
717  
718  
719  
720  
721  
722  
723  
724  
725  
726  
727  
728  
729  
730  
731  
732  
733  
734  
735  
736  
737  
738  
739  
740  
741  
742  
743  
744  
745  
746  
747  
748

sional forces on the actin core. This in turn may be coupled to the initiation of waves (Figure 6). Retrograde movement of MYO6+ was seen to occur in large patches (significantly brighter than a single molecule), as previously observed for MYO6 (34) and MYO15 (35), indicating that formation of large teams of motors is an important and conserved mechanism of motor regulation.

*Actin organization by other motors*

Why do filopodia form at the plasma membrane? Similar observations of motor translocation to the tips of filopodia have been made when expressing other plus-ended myosins such as MYO10 (12), MYO7A (13), MYO3 (36) and MYO15 (37). MYO19 is even capable of translating mitochondria to the tips of filopodia (38). Taken together, our data and these reports indicate that formation of filopodia, or at least condensation of actin filaments, may a general property of multimeric plus-ended myosins that must be regulated by cells. We speculate that one factor allowing growth of filopodia in the MYO6+ system is the protection of actin filaments from severing factors (e.g. gelsolin, villin, severin) and depolymerising factors (ADF/cofilin), caused by sequestration of F-actin away from the cytosol and into filopodia. It is interesting to note that despite much investigation of the mechanisms underlying filopodia formation by MYO10, a

similar phenomenon can be generated by a motor that is usually not associated with this process and is thus unlikely to contain any specific structural adaptations. Filopodia formation thus appears to be a universal property for multimeric plus-end directed myosins.

In conclusion, we have shown that reversing the direction of MYO6 leads to the reorganization of peripheral actin and endosomes. This adds to the list of situations in which MYO6 has been shown to affect actin organization. Many questions remain about the interaction of MYO6 with actin in its numerous functions, which will be probed in concert with the development of novel tools and methods.

**Materials and Methods**

MYO6+ was cloned by overlap extension PCR as described in the SI Materials and Methods. Details of cell culture, western blotting and all reagents used or generated can be found in the SI Materials and Methods. Details of sample preparation, structured illumination, confocal, TIRF and widefield microscopy and image analysis are described in the SI Materials and Methods.

**Acknowledgements**

We thank Justin Molloy and John Kendrick-Jones for critical reading of the manuscript. This work was supported by a BBSRC project grant (BB/K001981/1) awarded to FB. CIMR is supported by the Wellcome Trust with a strategic award (100140) and equipment grant (093026).

1. Lister I, et al. (2004) A monomeric myosin VI with a large working stroke. *Embo J* 23(8):1729-1738.

2. Phichith D, et al. (2009) Cargo binding induces dimerization of myosin VI. *P Natl Acad Sci USA* 106(41):17320-17324.

3. Wells AL, et al. (1999) Myosin VI is an actin-based motor that moves backwards. *Nature* 401(6752):505-508.

4. Tumbarello DA, Kendrick-Jones J, & Buss F (2013) Myosin VI and its cargo adaptors - linking endocytosis and autophagy. *J Cell Sci* 126(12):2561-2570.

5. Mukherjee M, et al. (2009) Myosin VI Dimerization Triggers an Unfolding of a Three-Helix Bundle in Order to Extend Its Reach. *Mol Cell* 35(3):305-315.

6. Batters C, Brack D, Ellrich H, Averbek B, & Veigel C (2016) Calcium can mobilize and activate myosin-VI. *P Natl Acad Sci USA* 113(9):E1162-E1169.

7. Yu C, et al. (2009) Myosin VI Undergoes Cargo-Mediated Dimerization. *Cell* 138(3):537-548.

8. Aschenbrenner L, Lee T, & Hasson T (2002) Myosin-VI facilitates the translocation of endocytic vesicles from cell peripheries. *Mol Biol Cell* 13:458a-458a.

9. Mukherjee M, et al. (2014) Myosin VI Must Dimerize and Deploy Its Unusual Lever Arm in Order to Perform Its Cellular Roles. *Cell Rep* 8(5):1522-1532.

10. Park H, et al. (2007) The unique insert at the end of the myosin VI motor is the sole determinant of directionality. *P Natl Acad Sci USA* 104(3):778-783.

11. Mattila PK & Lappalainen P (2008) Filopodia: molecular architecture and cellular functions. *Nat Rev Mol Cell Bio* 9(6):446-454.

12. Bohil AB, Robertson BW, & Cheney RE (2006) Myosin-X is a molecular motor that functions in filopodia formation. *P Natl Acad Sci USA* 103(33):12411-12416.

13. Sakai T, Umeki N, Ikebe R, & Ikebe M (2011) Cargo binding activates myosin VIIA motor function in cells. *P Natl Acad Sci USA* 108(17):7028-7033.

14. Husainy AN, Morrow AA, Perkins TJ, & Lee JM (2010) Robust patterns in the stochastic organization of filopodia. *Bmc Cell Biol* 11.

15. Loewenstein Y, Kuras A, & Rumpel S (2011) Multiplicative Dynamics Underlie the Emergence of the Log-Normal Distribution of Spine Sizes in the Neocortex In Vivo. *J Neurosci* 31(26):9481-9488.

16. Arden SD, Tumbarello DA, Butt T, Kendrick-Jones J, & Buss F (2016) Loss of cargo binding in the human myosin VI deafness mutant (R1166X) leads to increased actin filament binding. *Biochemical Journal* 473(19):3307-3319.

17. Naccache SN, Hasson T, & Horowitz A (2006) Binding of internalized receptors to the PDZ domain of GIPC/synectin recruits myosin VI to endocytic vesicles (vol 103, pg 12735, 2006). *P Natl Acad Sci USA* 103(41):15272-15272.

18. Tumbarello DA, et al. (2012) Autophagy-receptors link myosin VI to autophagosomes to mediate Tom1-dependent autophagosome maturation and fusion with the lysosome. *Mol Biol Cell* 23.

19. Morriswood B, et al. (2007) T6BP and NDP52 are myosin VI binding partners with potential roles in cytokine signalling and cell adhesion. *J Cell Sci* 120(15):2574-2585.

20. Majewski L, Sobczak M, Havrylov S, Jozwiak J, & Redowicz MJ (2012) Dock7: A GEF for Rho-family GTPases and a novel myosin VI-binding partner in neuronal PC12 cells. *Biochem Cell Biol* 90(4):565-574.

21. Sahlender DA, et al. (2005) Optineurin links myosin VI to the Golgi complex and is involved in Golgi organization and exocytosis. *J Cell Biol* 169(2):285-295.

22. Pylypenko O, et al. (2015) Myosin VI deafness mutation prevents the initiation of processive runs on actin. *P Natl Acad Sci USA* 112(11):E1201-E1209.

23. Buss F, et al. (1998) The localization of myosin VI at the Golgi complex and leading edge of fibroblasts and its phosphorylation and recruitment into membrane ruffles of A431 cells after growth factor stimulation. *J Cell Biol* 143(6):1535-1545.

24. Mallavarapu A & Mitchison T (1999) Regulated actin cytoskeleton assembly at filopodium tips controls their extension and retraction. *J Cell Biol* 146(5):1097-1106.

25. Altman D, Goswami D, Hasson T, Spudich JA, & Mayor S (2007) Precise positioning of myosin VI on Endocytic vesicles in vivo. *Plos Biol* 5(8):1712-1722.

26. Reymann AC, et al. (2012) Actin Network Architecture Can Determine Myosin Motor Activity. *Science* 336(6086):1310-1314.

27. Noguchi T, Lenartowska M, & Miller KG (2006) Myosin VI stabilizes an actin network during Drosophila spermatid individualization. *Mol Biol Cell* 17(6):2559-2571.

28. Mangold S, et al. (2011) Hepatocyte Growth Factor Acutely Perturbs Actin Filament Anchorage at the Epithelial Zonula Adherens. *Curr Biol* 21(6):503-507.

29. Loubery S, Delevoe C, Louvard D, Raposo G, & Coudrier E (2012) Myosin VI Regulates Actin Dynamics and Melanosome Biogenesis. *Traffic* 13(5):665-680.

30. Charizopoulou N, et al. (2011) Gipc3 mutations associated with audiogenic seizures and sensorineural hearing loss in mouse and human. *Nat Commun* 2:201.

31. Gunning PW, Hardeman EC, Lappalainen P, & Mulvihill DP (2015) Tropomyosin - master regulator of actin filament function in the cytoskeleton. *J Cell Sci* 128(16):2965-2974.

32. Leijnse N, Oddershede LB, & Bendix PM (2015) Helical buckling of actin inside filopodia generates traction. *P Natl Acad Sci USA* 112(1):136-141.

33. Sun YJ, et al. (2007) Myosin VI walks "Wiggly" on actin with large and variable tilting. *Mol Cell* 28(6):954-964.

34. Reed BC, et al. (2005) GLUT1CBP(TIP2/GIPC1) interactions with GLUT1 and myosin VI: Evidence supporting an adapter function for GLUT1CBP. *Mol Biol Cell* 16(9):4183-4201.

35. Yochelis A, et al. (2015) Self-organization of waves and pulse trains by molecular motors in cellular protrusions. *Sci Rep* 5:13521.

36. Les Erickson F, Corsa AC, Dose AC, & Burnside B (2003) Localization of a class III myosin to filopodia tips in transfected HeLa cells requires an actin-binding site in its tail domain. *Mol Biol Cell* 14(10):4173-4180.

37. Liu R, et al. (2008) Sisypheus, the Drosophila myosin XV homolog, traffics within filopodia transporting key sensory and adhesion cargos. *Development* 135(1):53-63.

38. Shneyer BI, Usaj M, & Henn A (2016) Myo19 is an outer mitochondrial membrane motor and effector of starvation-induced filopodia. *J Cell Sci* 129(3):543-556.

39. Bennett RD, Mauer AS, & Strehler EE (2007) Calmodulin-like protein increases filopodia-dependent cell motility via up-regulation of myosin-10. *J Biol Chem* 282(5):3205-3212.

40. Chibalina MV, Seaman MNJ, Miller CC, Kendrick-Jones J, & Buss F (2007) Myosin VI and its interacting protein LMTK2 regulate tubule formation and transport to the endocytic recycling compartment. *J Cell Sci* 120(24):4278-4288.

41. Spudich G, et al. (2007) Myosin VI targeting to clathrin-coated structures and dimerization is mediated by binding to disabled-2 and PtdIns(4,5)P-2. *Nat Cell Biol* 9(2):176-U167.

42. De la Cruz EM, Ostap EM, & Sweeney HL (2001) Kinetic mechanism and regulation of myosin VI. *J Biol Chem* 276(34):32373-32381.

43. Arjonen A, et al. (2014) Mutant p53-associated myosin-X upregulation promotes breast cancer invasion and metastasis. *J Clin Invest* 124(3):1069-1082.

749  
750  
751  
752  
753  
754  
755  
756  
757  
758  
759  
760  
761  
762  
763  
764  
765  
766  
767  
768  
769  
770  
771  
772  
773  
774  
775  
776  
777  
778  
779  
780  
781  
782  
783  
784  
785  
786  
787  
788  
789  
790  
791  
792  
793  
794  
795  
796  
797  
798  
799  
800  
801  
802  
803  
804  
805  
806  
807  
808  
809  
810  
811  
812  
813  
814  
815  
816

Please review all the figures in this paginated PDF and check if the figure size is appropriate to allow reading of the text in the figure.

If readability needs to be improved then resize the figure again in 'Figure sizing' interface of Article Sizing Tool.